Electronic Supplementary Material (ESI) for Chemical Science.

Supporting Information

Specific Protein Labeling with Caged Fluorophores for Dual-Color Imaging and Super-Resolution Microscopy in Living Cells

Sebastian Hauke, Alexander von Appen, Tooba Quidwai, Jonas Ries
and Richard Wombacher*

Content

1. General remarks

Unless otherwise stated, all chemicals were purchased from commercial sources (ABCR, AnalaR, Grüssing). Commercially available chemical reagents were of analytical grade and used without further purification. Moisture-sensitive reactions were conducted under constant argon atmosphere in dried, heated, baked-out glass ware. Organic solvents were removed under reduced pressure, utilizing a rotary evaporator. Residual solvent was removed under high-vacuum for a minimum of 24 h.

Analytical thin layer chromatography

The reaction progress was monitored via analytical TLC which was performed on Macherey-Nagel Polygam® $SILUV_{254}$ plastic-sustained pre-coated silica plates. Components were visualized by observation under UV irradiation (254 nm and 365 nm) or with aqueous $KMnO_4$ solution or via blue shift staining reagent (cerium molybdate), followed by heat treatment.

Analytical and semi-preparative high-pressure liquid chromatography (HPLC)

Analytical HPLC (Phenomenex Luna C-18 (100 × 4.6 mm) and Agilent Poroshell 120 SB C-18 (100 × 4.60 mm, 2.7 micron) analysis was performed on an Agilent 1100 Series HPLC system, equipped with a diode array and a fluorescence detector. A gradient of 0.1% TFA in water and 0.1% TFA in acetonitrile at 1.0 ml/min flow was applied for elution. Semi-preparative HPLC (Phenomenex Luna C-18, 15.00 × 250 mm) used the same gradient at a flow rate of 5 ml/min. Methods were performed within 80 min. Data evaluation was performed via ChemStation 3D (Agilent) and Origin 8.5.1 (OriginLab) software.

Nuclear magnetic resonance (NMR)

NMR spectra were recorded at RT on Varian Mercury Plus 500 MHz spectrometer. Chemical shifts are reported in parts per million (ppm) relative to residual un-deuterated solvent peak, coupling constants are given in Hz. The following abbreviations are used to indicate the signal multiplicity: s (singlet), d (doublet), t (triplet), q (quartet), m (multiplet), dd (doublet of doublet). All NMR spectra were integrated and processed using MestreNova software. ^{1}H-NMR spectra of all herein synthesized compounds are given in the ESI.

High-performance liquid chromatography coupled mass spectrometry (HPLC-MS)

High-resolution (HR) mass spectrometry was conducted on a Bruker mircOTOF II 10254 mass spectrometer. The preceding LC step was conducted on an Agilent 1200 HPLC system (Phenomenex C-18, 200 x 2.1 mm, 3 micron), equipped with a multi-wavelength detector. Flow rates were adjusted to 200 µl/min. A gradient of 0.1% formic acid in water (pH 3) and 0.1% formic acid in acetonitrile was used for elution. Full scan single mass spectra were recorded in ranges of m/z = 200 – 3000. Calculated molecular weights refer to the m/z values given by the Hyphenation Star PP (Version 3.2.44.1) and DataAnalysis ESI-compass 1.3 (Version 4.0) data analysis software tools (Bruker Daltonics). Deconvolution of mass spectra was accomplished via Maximum Entropy

Deconvolution. High-resolution mass spectra were obtained utilizing ESI Tunemix (Fluka) for calibration.

2. Synthesis of photoactivatable fluorophores and conjugates

Trimethoprim modified with an amine bearing ethylene glycole linker (TMP-$(PEG)_3$-NH_2) **(2)**, TMP-tetra-methyl-rhodamine (TMP-TMR) and TMP-di-acetyl-fluorescein (TMP-diAcFl) were synthesized according literature procedures [1]. Halo-$(PEG)_3$ amine **(1),** Halo-TMR and Halo-diAcFl were synthesized following the described procedure from G. V. Los *et al.* [2]. di-*ortho*-nitrophenyl-5-carboxy-fluorescein was synthesized according literature [3].

TMP-PA-Fluorescein (3)

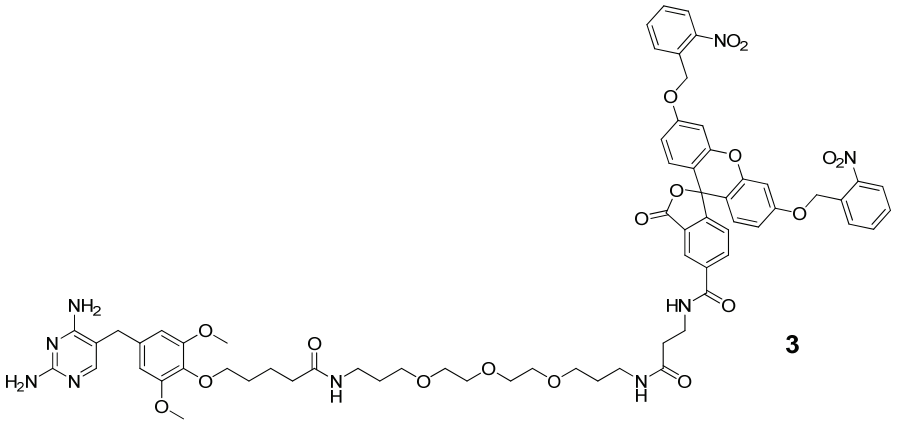

3

di-*ortho*-nitrophenyl-5-carboxy-fluorescein [3] (4 mg, 3.13 µmole) was dissolved in dry DMF (500 µl) in a 25 ml Schlenk flask on ice. A solution of (2-(6-Chloro-1H-benzotriazole-1-yl)-1,1,3,3-tetramethylaminium hexafluorophosphate) (HCTU, 2.3 mg, 1.5 eq.) in dry DMF (250 µl) was added dropwise under Ar in the dark. Triethylamine (2 µl) was added and the mixture was stirred on ice for 10 min. TMP-PEG3-NH_2 **(2)** (4.7 µmole, 1.5 eq.) was added stepwise together with triethylamine (1 µl). The reaction progress was followed via thin layer chromatography (TLC) (DCM:MeOH 10:1). After stirring on ice for 1 h, the reaction mixture was allowed to reach RT under Ar in the dark, over night. The solvent was evaporated under reduced pressure. The crude product was purified via semi-preparative HPLC (RP-18, MeCN / H_2O, 1% TFA, gradient 10-65% in 60 min) to afford a colorless solid, after lyophilization.

^{1}H-NMR (400 MHz, Methanol-d_4) δ 8.41 (dd, *J* = 1.6, 0.8 Hz, 1H), 8.18 (dd, *J* = 8.1, 1.6 Hz, 1H), 8.12 (dd, *J* = 8.2, 1.3 Hz, 2H), 7.82 (dd, *J* = 7.6, 1.1 Hz, 2H), 7.73 (td, *J* = 7.6, 1.3 Hz, 2H), 7.57 (ddd, *J* = 8.2, 7.4, 1.5 Hz, 2H), 7.30 (dd, *J* = 8.0, 0.7 Hz, 1H), 7.27 – 7.22 (m, 1H), 6.96 (d, *J* = 2.5 Hz, 2H), 6.78 (dd, *J* = 8.9, 2.5 Hz, 2H), 6.73 (d, *J* = 8.8 Hz, 2H), 6.53 (s, 2H), 5.52 (s, 4H), 3.90 (t, *J* = 6.1 Hz, 2H), 3.78 (s, 6H), 3.69 (t, *J* = 6.7 Hz, 2H), 3.66 (s, 2H), 3.62 – 3.57 (m, 4H), 3.57 – 3.46 (m, 10H), 3.28 (t, *J* = 6.8 Hz, 2H), 3.24 (t, *J* = 6.9 Hz, 2H), 2.55 (t, *J* = 6.7 Hz, 2H), 2.23 (t, *J* = 7.3 Hz, 2H), 1.81 – 1.65 (m, 8H).

HR MS (ESI pos.) m/z: calculated for [$C_{66}H_{73}N_9O_{18}$] 1278.4990 [M+H^+], measured: 1278.5002.
Yield: 90%

Halo-PA-Q--Rhodamine (4)

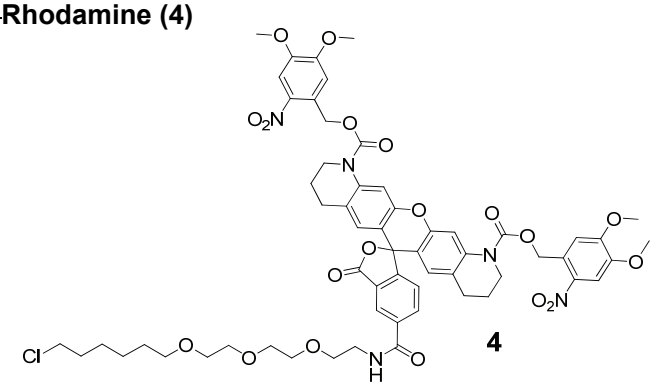

4

NVOC2-5-carboxy-Q-rhodamine (2.5 mg, 2.7 µmole) was dissolved in dry DMF (500 µl) in a 25 ml Schlenk flask on ice. A solution of (2-(6-Chloro-1H-benzotriazole-1-yl)-1,1,3,3-tetramethylaminium hexafluorophosphate) (HCTU, 2 mg, 1.5 eq.) in dry DMF (250 µl) was added dropwise under Ar in the dark. Triethylamine (2 µl, 1.5 eq.) was added and the mixture was stirred on ice for 10 min. Halo-PEG3-NH_2 **(1)** (4.1 µmole, 1.5 eq.) was added stepwise together with triethylamine (0.6 µl, 0.5 eq.). The reaction progress was followed via thin layer chromatography (TLC) (DCM:MeOH 10:1). After stirring of on ice for 1 h, the mixture was allowed to reach RT under Ar in the dark, over night. The solvent was evaporated under reduced pressure. The crude product was purified via semi-preparative HPLC (RP-18, MeCN / H_2O, 1% TFA, gradient 10-65% in 60 min) to afford a colorless solid, after lyophilization.

^{1}H-NMR (500 MHz, Methanol-d_4) δ 8.47 (dd, *J* = 1.6, 0.8 Hz, 1H), 8.23 (dd, *J* = 8.1, 1.6 Hz, 1H), 7.77 (s, 2H), 7.76 (s, 2H), 7.31 (dd, *J* = 8.0, 0.7 Hz, 1H), 7.16 (s, 2H), 6.56 (s, 2H), 5.65, 5.61 (ABq, *J* = 14.4 Hz, 4H), 5.34 (t, *J* = 4.9 Hz, NH), 3.90 (s, 6H), 3.87 – 3.75 (m, 4H), 3.85 (s, 6H), 3.71 (t, *J* = 5.4 Hz, 2H), 3.68 (s, 4H), 3.66 – 3.62 (m, 4H), 3.57 – 3.54 (m, 2H), 3.49 (t, *J* = 6.7 Hz, 2H), 3.42 (t, *J* = 6.6 Hz, 2H), 2.70 – 2.62 (m, 2H), 2.61 – 2.53 (m, 2H), 2.21 – 2.17 (m, 2H), 1.92 – 1.86 (m, 4H), 1.73 – 1.66 (m, 2H), 1.52 (m, 2H), 1.39 – 1.29 (m, 2H).

HR MS (ESI pos.) m/z: calculated for [$C_{59}H_{65}ClN_5O_{19}$]: 1182.3957 [M+H^+], measured: 1182.3945.
Yield: 95.3%

TMP-PA-Q-Rhodamine (5)

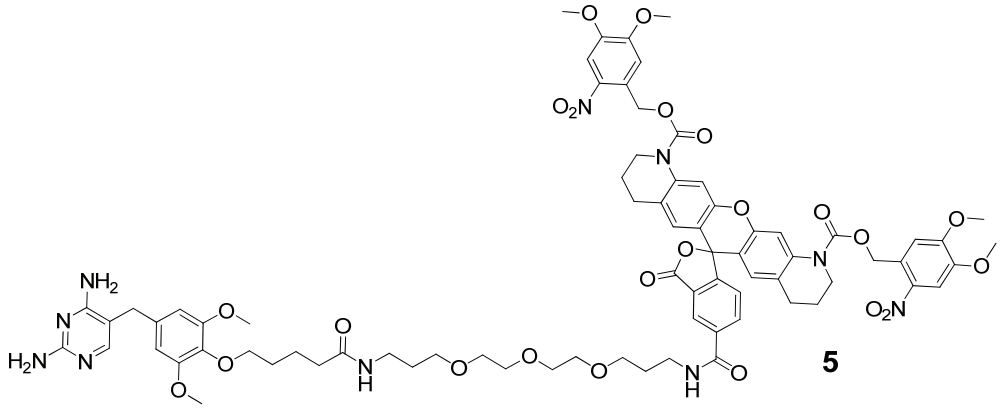

5

NVOC2-5-carboxy-Q-rhodamine (2.5 mg, 2.7 µmol) was dissolved in dry DMF (500 µl) in a 25 ml Schlenk flask on ice. A solution of (2-(6-Chloro-1H-benzotriazole-1-yl)-1,1,3,3-tetramethylaminium hexafluorophosphate) (HCTU, 2 mg, 1.5 eq.) in dry DMF (250 µl) was added dropwise under Ar in the dark. Triethylamine (2 µl, 1.5 eq.) was added and the mixture was stirred on ice for 10 min. TMP-PEG3-NH_2 **(2)** (4.1 µmol, 1.5 eq.) was added stepwise together with triethylamine (0.6 µl, 0.5 eq.). After stirring of on ice for 1 h, the mixture was allowed to reach RT under Ar in the dark, over night. The reaction progress was followed via TLC (DCM:MeOH 10:1). The solvent was evaporated under reduced pressure. The crude product was purified via semi-preparative HPLC (RP-18, MeCN / H_2O, 1% TFA, gradient 10-65% in 60 min) to afford a colorless solid after lyophilization.

^{1}H-NMR (500 MHz, Methanol-d_4) δ 8.69 (t, *J* = 5.6 Hz, NH), 8.45 – 8.42 (m, 1H), 8.21 (dd, *J* = 8.1, 1.6 Hz, 1H), 7.75 (s, 2H), 7.74 (s, 2H), 7.31 (d, *J* = 8.0 Hz, 1H), 7.23 (d, *J* = 1.1 Hz, 1H), 7.14 (s, 2H), 6.55 (s, 2H), 6.51 (s, 2H), 5.62, 5.57 (ABq, *J* = 14.4 Hz, 4H), 5.34 (t, *J* = 4.9 Hz, NH), 3.89 (s, 6H), 3.86 – 3.72 (m, 8H), 3.85 (s, 6H), 3.73 (s, 6H), 3.68 – 3.56 (m, 12H), 3.55 – 3.53 (m, 4H), 3.47 (t, *J* = 6.1 Hz, 2H), 3.22 (t, *J* = 6.9 Hz, 2H), 2.68 – 2.59 (m, 2H), 2.59 – 2.52 (m, 2H), 2.23 – 2.19 (m, 2H), 1.95 – 1.90 (m, 2H), 1.79 – 1.56 (m, 6H).

HR MS (ESI pos.) m/z: calculated for [$C_{75}H_{85}N_{10}O_{23}$]: 1493.5784 [$M+H^+$], measured: 747.2934 (z = 2) and 1493.6242 (z = 1).

Yield: 96.8%

3. ^{1}H-NMR spectra

TMP-PA-Fluorescein (**3**)

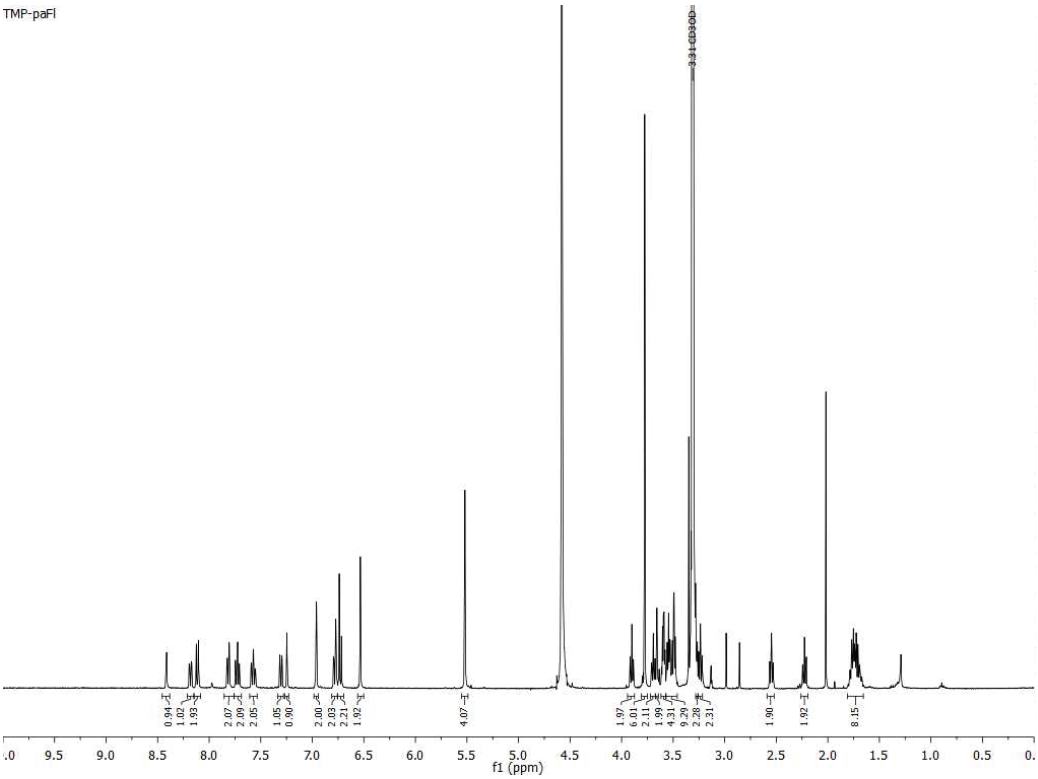

Halo-PA-Q-Rhodamine (**4**)

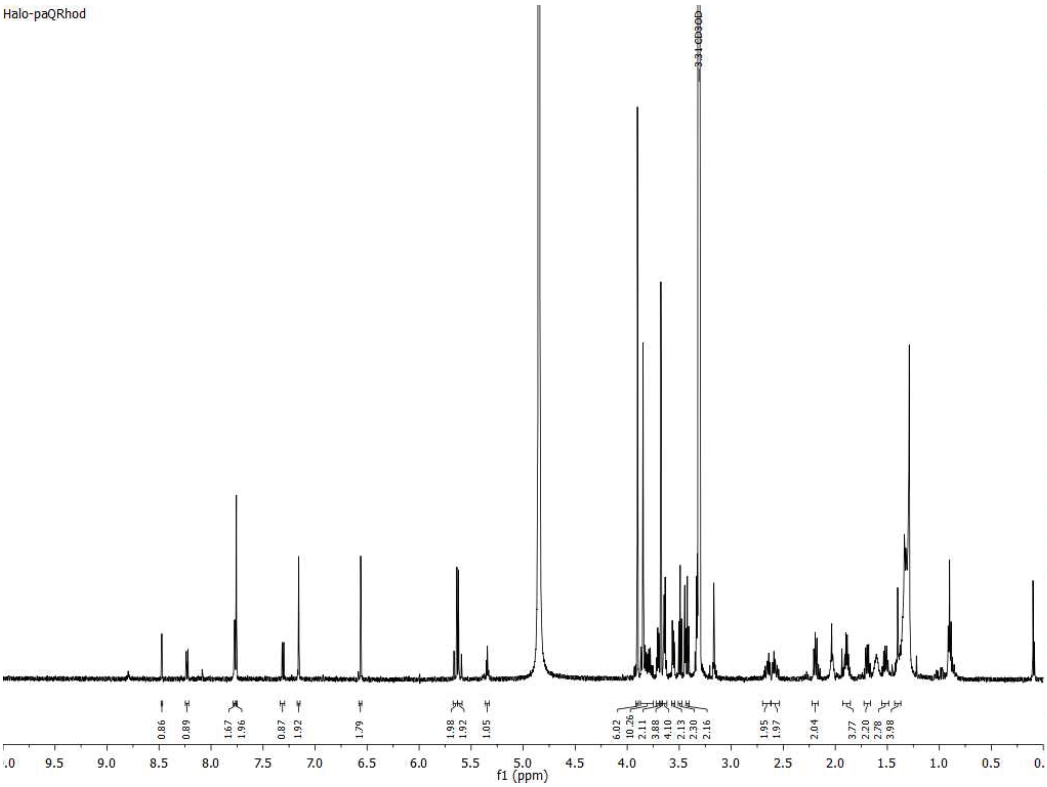

TMP-PA-Q-Rhodamine (**5**)

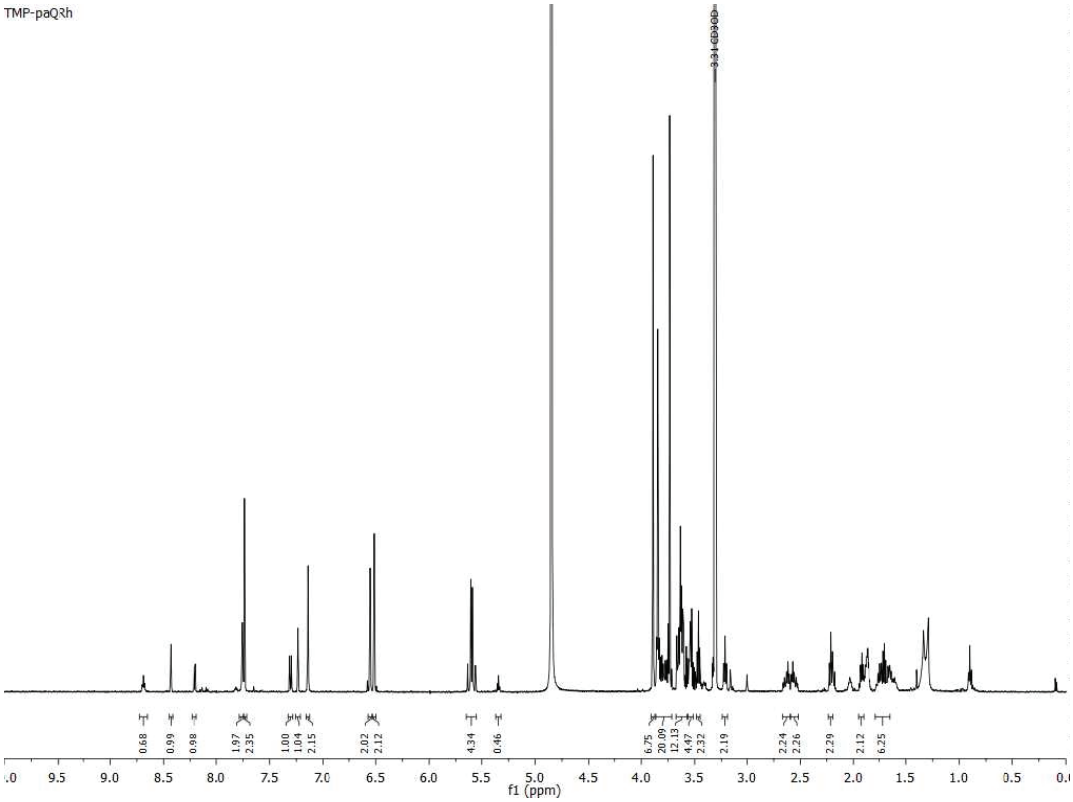

HPLC chromatograms of (A) TMP-PA-Fl and (B) TMP-PA-Q-Rh:

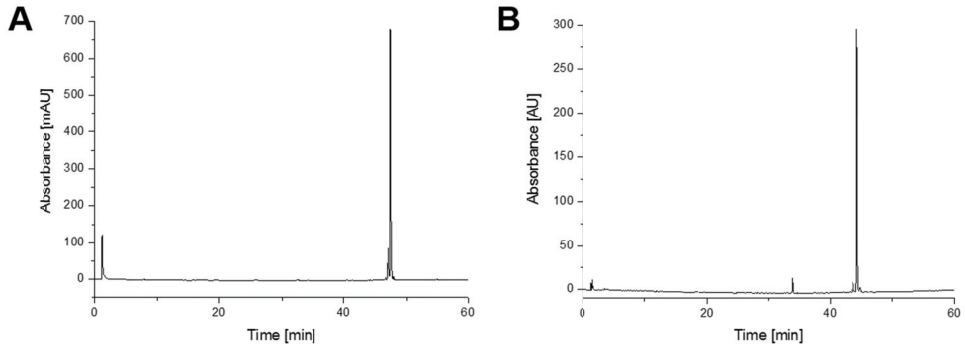

4. Fluorescence spectra – *in vitro* activation of caged fluorophore conjugates

In advance of live cell photoactivation experiments, caged Q-rhodamine (NVOC2-5-carboxy-Q-rhodamine) and caged fluorescein (spectral properties of fluorophores are summarized in Table S1) were investigated for their photoactivation properties *in vitro*. For this, 5 µM solutions (diluted in water) of the respective caged fluorophores were prepared. *In vitro* photoactivation experiments were conducted in an UV cabinet (Alpha Imager image analysis system 2200), equipped with 8 W UV-tubes (λ = 365 nm). To exclude high-energy light (λ < 300 nm), the cuvettes were placed on polytheylene petri-dishes (with a cut-off, determined at λ = 300 nm). To minimize the influence of heat that was emitted from the UV-tubes on the photoactivation reaction, cuvettes were covered

with ice. Photoactivation of fluorescence was monitored using a JASCO Spectrofluorometer FP-6500 utilizing 15 µl Teflon-capped quartz cuvettes (layer thickness: 1.5 mm, Hellma analytics, Germany). Fluorescence emission was detected in intervals of λ_{em} = 515 – 700 nm for caged Q-rhodamine and λ_{em} = 494 – 700 nm for caged fluorescein. The scanning speed was set to 500 nm/min. The turn-on of fluorescence upon photoactivation was calculated based on determined areas under the curves. All measurements were conducted in triplicates. For data evaluation, Origin 8.5.1 (OriginLab) was applied.

Table S1: Overview of spectral properties of applied fluorochromes.

Fluorochrome	Excitation maximum [nm]	Emission maximum [nm]	Photoactivation at [nm]	Color of spectral class	References
Diacetyl fluorescein	485	514	-	green	[4,5]
Tetramethylrhodamine	540	565	-	red	[4–7]
(PA) fluorescein	497	516	300 - 400	green	[8,9]
(PA) Q-rhodamine	537	556	350, 405, 420	red	Sigma-Aldrich,[10]
EGFP	489	509	-	green	[11–14]
mCherry	587	610	-	red	[15]
pmTurquoise2	435	475	-	green	[16]

5. Construct design and preparation

Primer sequences of 17-35 nucleotides were designed, with synthesis and delivery by Integrated DNA Technologies, Inc. (IDT, Belgium). DNA modification was monitored via standard agarose gel electrophoresis, applying appropriate agarose concentrations. DNA plasmids were amplified in *E. coli* (strain: DH5α) in selective LB-medium. Plasmid purification was performed utilizing the commercial systems GeneJet Plasmid Miniprep Kit or QUIAGEN Plasmid Maxi Kit. Gel extraction was conducted using the QIAquick Gel Extraction Kit, following the guidelines of the manufacturers. DNA concentrations and purities were checked via UV-Vis spectrometry, utilizing a NanoDrop-2000 system. Sanger sequencing was ordered from Sequence Laboratories Göttingen (Seqlab, Germany) utilizing standard sequencing primers.

Tom20-eDHFR and H2B-eDHFR plasmid vectors were kindly provided by Virginia W. Cornish (Columbia University) [17]. Halo-EGFP-Vcl and eDHFR-EGFP-Vcl were a gift from Dirk Ollech (Heidelberg University). Tom20-Halo was generated using the FlexiVector cloning kit (Promega). We first amplified the Tom20 sequence from a Tom20-hAGT vector (gift from Covalys) using SgfI and PmeI flanked primers (ATTGCGATCGCCAAGCTCGAAATTAACCCTCAC and TTAGTTTAAACCTTCATTTCGCAGTCTTTGTCC). 500 ng of the purified PCR product was mixed with 20% *v/v* 5x Flexi Digest Buffer and 20% *v/v* Flexi Enzyme Blend (SgfI/PmeI) to a final volume of 20 µl and incubated for 30 min at 37°C for restriction digest followed by 20 min at 65°C heat deactivation. 200 ng of the Halo-tag containing vector pFN21A (Promega) was linearized by mixing with 20% *v/v* 5x Flexi Digest Buffer and 10% *v/v* Flexi Enzyme Blend (SgfI/PmeI) to a final volume of 20 µl and incubating for 30 min at 3°C followed by 20 min at 65°C heat deactivation. For ligation, 40 ng digested and purified PCR fragment and 50 ng linearized vector were incubated for 80 min at

RT with 50% *v/v* Flexi Ligase Buffer and 20 U T4 DNA Ligase in a final volume of 20 µl. Unless otherwise noted all materials were included in the HaloTag Cloning Starter System Kit. Cloning of Halo-H2A and Halo-H2B was performed based on commercially available FlexiVectors® (Promega GmbH, Germany), following the guidelines of the manufacturer. For the generation of H2A-Halo, H2A-pmTurquoise was received from the Addgene platform (plasmid#36207). The protein-coding inserts were amplified from template vectors via PCR. PCR primers were designed in a way to introduce recognition sites for rare-cutting restriction endonucleases *SgfI* and *PmeI* at the respective ends of the POI-encoding sequence. Here, the SgfI recognition site was introduced upstream of the start codon, whereas the PmeI site was designed to contain the stop codon for the coding sequence. A single valine amino acid residue was attached to the carboxy-terminus of the protein. (PCR-primer: Halo-H2B *SgfI* forward ATTGCGATCGCCATGCCTGAACCCTCTAAGTCTGCTC, Halo-H2B *PmeI* reverse TTATGTTTAAACCTTAGAGCTAGTGTACTTGGTAACTGCCTTAGTG with H2B-eDHFR template and HaloH2A *SgfI* forward ATTGCGATCGCCATGTCGGGACGCGGCAAGCAG, HaloH2A *PmeI* reverse TTATGTTTAAACTTTGCCTTTGGCCTTGTGGTG with pmTurquoise2-H2A template) PCRs were performed following standard protocols and checked via agarose gel electrophoresis, conducted according to the standard protocols. For digestion of designed inserts with SgfI and PmeI endonucleases, 0.5 µg of the purified PCR product were mixed with 20% v/v Flexi®Enzyme Blend (PmeI/SgfI) and 20% v/v 5× Flexi®Digest Buffer to a final volume of 20 µl. Digestion at 37°C for 30 min was directly followed by heat inactivation at 65°C for 20 min. For ligation, 100 ng of digested PCR fragments were added to 60 ng of linearized target vector (pFN21A), 20 U T4 DNA ligase and 50% v/v Flexi®Ligase Buffer (final volume: 20 µl). The ligation reaction was conducted at RT within 120 min. The overall cloning procedure was finally monitored via agarose gel electrophoresis (1% agarose). For amplification, cloned plasmids were transformed into chemically competent bacteria cells (*E. coli* DH5α) according to the standard protocols. Successful cloning was confirmed via Sanger sequencing.

6. Cell culture and sample preparation for imaging

COS-7, NIH 3T3 and MEF $Vcl^{-/-}$ mammalian cells were maintained in DMEM (Gibco, 1 g/l glucose, supplemented with 10% v/v fetal bovine serum (FBS)) at 37°C in a 5% high humidity CO_2 atmosphere in 25 cm^2 tissue culture flasks. Splitting was performed as adherent cells reached confluence of 70-80%. For this, standard protocols were applied, utilizing 0.05% w/v pre-warmed Trypsin-EDTA (Gibco) solution.

For seeding of cells for live cell imaging experiments, the density of cell suspensions was determined using a Neubauer hematocytometer (0.0025 mm^2). For epifluorescence imaging, cell suspensions were adjusted to 70 cells/µl. 30 µl of the respective dilutions were plated per channel of an Ibidi µ-Slide $VI^{0.4}$. The cells were allowed to attach for 1 h at 37°C. Then, 60 µl DMEM (+ 10% FBS) were added gently to each reservoir of the µ-Slide. That way, monolayers of cells (60 - 70% confluence) were obtained which were incubated for 24 h under standard conditions in advance of transfection. For transient transfection of cells, 1-to-3 ratios of microliter-reagent to microgram-

plasmid DNA were applied, following the instructions of the suppliers (X-tremeGene HP, Roche, Fugene Promega).

In advance of fluorescent staining of mammalian cells, the old growth medium containing the transfection reagent was aspirated. Cells were gently washed three times with pre-warmed growth medium to remove residual transfection reagent. The (caged) fluorescent conjugates were prepared as stocks in DMF. The final concentration of DMF on cells was less than 0.1%. For application to cells, (caged) fluorescent dyes were prepared as solutions in growth medium from the stocks. PA dyes were supplied to cells in final concentrations of 5 µM, non-PA dyes in 1 µM concentration. For optimal labeling efficiencies, cells were incubated with the labeling mixture for 45 min (TMP-fluorophores) and 3.5 h (Halo-fluorophores). Following staining of cells, the staining mixture containing the fluorescent dyes was removed and the cells were gently washed twice with growth medium and DPBS and incubated for additional 45 min in growth medium (standard conditions) to allow the dissociation of unbound fluorophores.

Cell viability assay

Cell viability after incubation with presented dye-conjugates was checked using *Promega CellTiter 96 one solution cell proliferation assay* (Results se figure S15). For this, the human cancer cell line HeLa was tested as a standard cell line in the scientific community, as well as NIH 3T3 mouse fibroblasts, which found application in the presented work. 10^4 cells were seeded in each well of a *Thermo Scientific Nunclon 95-well plate*. Cells were incubated 12 h at 37°C and 5% CO_2 in humidified atmosphere in advance of the experiment. Cells were treated with 5 µM of the (caged) fluorophore conjugates (standard staining conditions). The assay was performed following the manufacturer´s guidelines.

7. Diffraction-limited fluorescence microscopy

Epifluorescence microscopy

Epifluorescence microscopy was performed on a Zeiss Axio Observer.Z1 inverted microscope, using Plan-Apochromat 40x (NA 1.3, oil) and Plan-Apochromat 63x (NA 1.49, oil) lenses, AxioCam MR3 CCD camera and Axiovision software; version 40 V 4.7.2. The red fluorescence channel was imaged using a 120 W HXP120 mercury arc lamp with a 562/40 excitation band pass. Fluorescence was collected utilizing a 624/40 emission filter. The green channel was imaged using aforementioned mercury halogen lamp with a 472/30 excitation filter and a GFP 520/35 HQ emission filter. Photoactivation experiments of caged Q-rhodamine and caged fluorescein in live cells were conducted by exposure of transfected and stained cells to light that passed the DAPI excitation filter 377/50 (14.5 mW/cm^2) through the objective of the wide-field microscope. Pre-exposure images were recorded, followed by exposure to UV light for the indicated time periods. After photoactivation, post-exposure images were acquired. For the determination of optimal periods of activation, selected ROIs were repetitively exposed to activation light in 5 s-intervals. For this, the shutter was opened and closed manually, followed by the acquisition of a frame. Finally, the intensity values of increasing fluorescence signal were compared.

Confocal laser scanning microscopy

Imaging was performed on an Olympus IX83 confocal laser scanning microscope using an Olympus Plan-APON 60x (NA 1.4, oil) objective. The images were acquired utilizing a Hamamatsu C9100-50 EM CCD camera. Image acquisition was performed via FluoView imaging software, version 4.2. The green channel was imaged using the 488 nm laser line (120 mW/cm^2) at 3% laser power and a 525/50 emission mirror. The red channel was imaged using the 559 nm laser (120 mW/cm^2) at 2.0% laser power and a 643/50 emission filter. A 405 nm laser line was applied for photoactivation experiments. For uncaging experiments, circular regions of interest (ROIs) of 4-10 µm diameter were pre-defined. Pre-activation images were captured for 5 frames (5s/frame), followed by 30 s of activation within the ROI. Recovery images were captured for 35 min at a frame rate of 5 s/frame.

Total Internal reflection microscopy

Total internal reflection microscopy (TIRF) was carried out on an Olympus Biosystems Cell^R inverted microscope, equipped with an Olympus Uapo N TIRF 100x (NA 1.49 oil) objective. The red channel was imaged using the 561 nm laser line, the green channel was acquired via the 488 nm laser. For photoactivation experiments, the 405 nm laser line was applied. Emission was recorded utilizing a 535/50 emission filter for the green channel and a 617/73 filter for the red channel. The images were recorded utilizing Hamamatsu C9100-50 EM CCD camera and xCELLence software (exposure: 200 ms). The imaging laser beams were directed towards the µ-slide so that they were totally internally reflected at the bottom of the µ-slide and exponentially relaxed into the solution near the water-plastic interface as evanescent light waves. The µ-slide and immersion oil were exactly matched in refractive index which was identical to the refractive index of glass. The fluorescence that was excited by the evanescent light wave was collected by the exciting objective. Collected scattered light was filtered by a conventional Semrock Di01-R405-488-561-635 25x36 dichroic mirror. As the optimal TIRF settings were found, illumination angles were set and applied for imaging in both channels. Photoactivation of caged Q-rhodamine in live cells was conducted by exposure of cells to light of the 405 nm laser line in epi-mode (60 mW/cm^2, 50%). Pre-activation images were acquired in both green and red- channels. For photoactivation, cells were exposed to activation light of the 405 nm laser. Images were recorded after photoactivation due to exposure of cells to activation light of the respective wavelengths (exposure time: 200 ms).

Image analysis

Image analysis was conducted utilizing Fiji open source image analysis software tool (utilizing the latest updates) [18]. Lookup tables (LUTs) were applied to match the color within the recorded image with the wavelengths of detected light. For comparability, the LUTs of pre- and postactivated images were set the same weighting.

8. Photoactivated localization microscopy (PALM)

Optical set up

Localization microscopy was performed on a custom-built microscope. Single-mode output from an iChrome MLE-L laser box equipped with 405 nm, 488 nm, 561 nm and 640 nm laser lines (Toptica Photonics) was focused onto the back-focal plane of a 60x NA 1.49 TIRF objective (Nikon) and adjusted for epi illumination.Emission light was filtered using FF01-446/523 multi bandpass filter Semrock), and focused by a 400 mm tube lens onto the chip of an EMCCD camera (Ixon Ultra, Andor). A piezo objective positioner (Physikinstrumente, Karlsruhe, Germany) was used to move the z-focus. The focus was stabilized by an electronic feedback loop based on an infrared laser that was totally internally reflected at the coverslip and detected by a quadrant photodiode. The z-stability was better than ±10 nm over several hours. System was equipped with a stage designed to minimize drift and further lateral drift, typically smaller than 50 nm/h, was corrected for in the analysis software.

Image acquisition

Live cell sample prepared in ibidi slides where mounted in a custom-made holder and covered with 120µl imaging buffer. The sample was illuminated at 561nm with approx. 1kW/cm^2. Acquisition was started after achieving single molecule blinking. The UV laser (405 nm) was adjusted to maintain a constant activation of 15 molecules/frame. 4000-5000 frames where acquired at a 20Hz frame rate using micromanager [19].

Localization analysis

Localization analysis was performed as described before [20]. Briefly, pixel counts were converted to photons by subtracting the constant offset and multiplying by the inverse gain. Approximate locations of bright spots in each image were determined by smoothing, non-maximum suppression and thresholding. Selected regions of interest were fitted by a pixelated Gaussian function and a homogeneous photonic background with a maximum likelihood estimator (MLE) for Poisson distributed data using a freely available, fast GPU fitting [21] on a GeForce GTX275 (Nvidia). Lateral drift was corrected based on the imaged features: blocks of typically 5,000 frames were used to reconstruct one PALM image. Displacements among all reconstructed images were determined by image correlation and fitting of the maximum with an elliptical Gaussian. Displacements corresponding to each time point were averaged using a robust estimator, interpolated by a spline and used to correct the position of each localization. From the variation of the spline, we estimate that the residual error for the corrected positions was about 2 nm. For fixed cells, localization bursts with a distance smaller than 90 nm in consecutive frames (interrupted by not more than two frames) were grouped into a single localization. Finally, localizations with an uncertainty of σmax > 10 nm (15 nm for live-cell imaging) were discarded. All analysis software was written in Matlab (Mathworks).

9. Supporting Figures

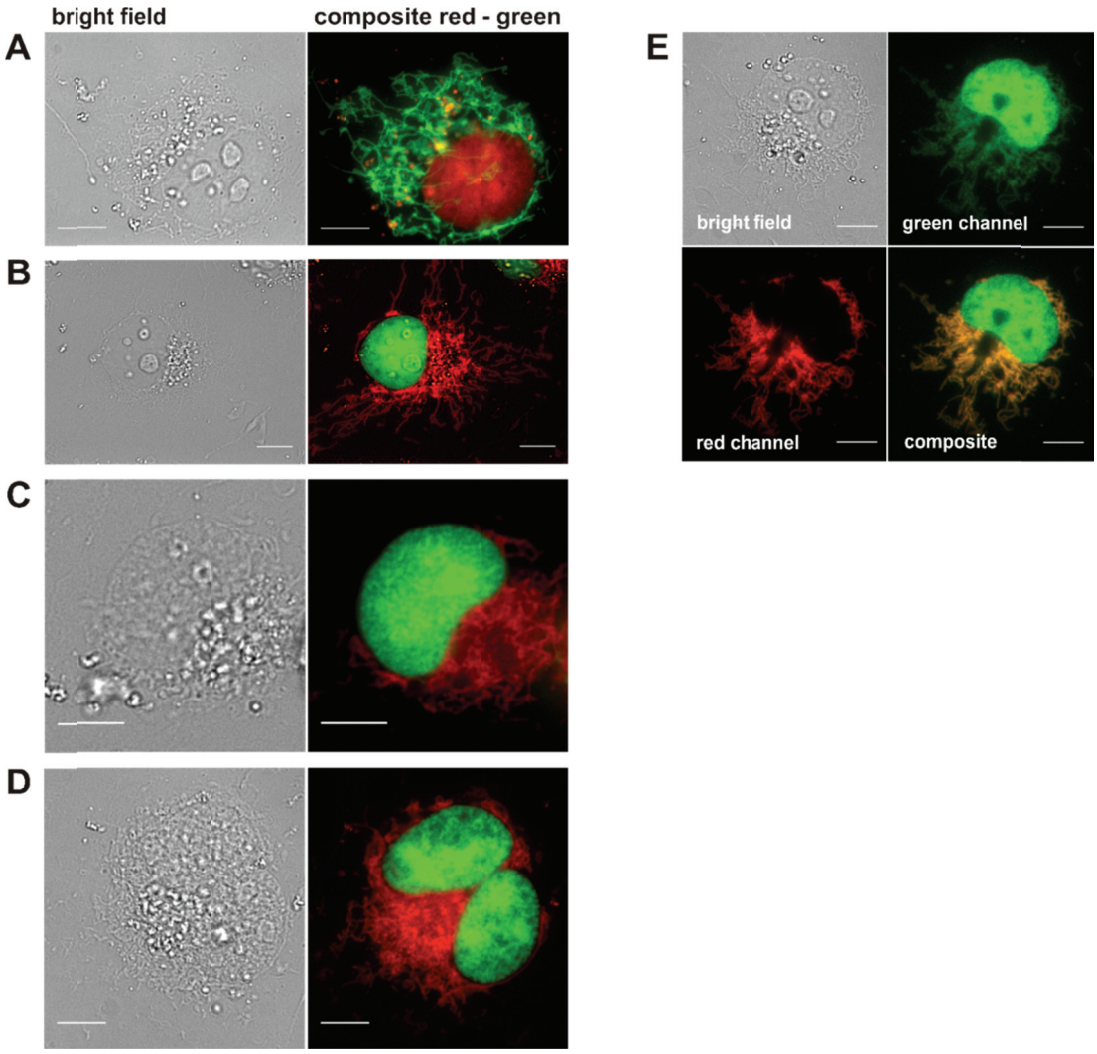

Figure S1. Monitoring FP-, Halo- and eDHFR-tagged mitochondrial and nuclear POIs to validate the properties of presented fluorophore conjugates inside live COS-7 cells. Imaging was performed on live COS-7 cells, following transient co-overexpression of **(A)** H2B-eDHFR and Tomm20-Halo (staining with TMP-TMR and Halo-diAcFl, 1 µM each), **(B)** H2B-Halo and Tomm20-eDHFR (staining with TMP-TMR and Halo-diAcFl, 1 µM each), **(C)** H2B-EGFP and Tomm20-Halo (staining with Halo-TMR, 1 µM), **(D)** H2B-EGFP and Tomm20-eDHFR (staining with TMP-TMR, 1 µM) and **(E)** H2B-Halo and Tomm20-mCherry-Halo (staining with Halo-diAcFl, 1 µM). Images were recorded utilizing 60x (A) or 40x (B - E) objectives and are represented as dual-color recordings (right panels). Bright field images are shown on the left. Scale bars: 10 µm.

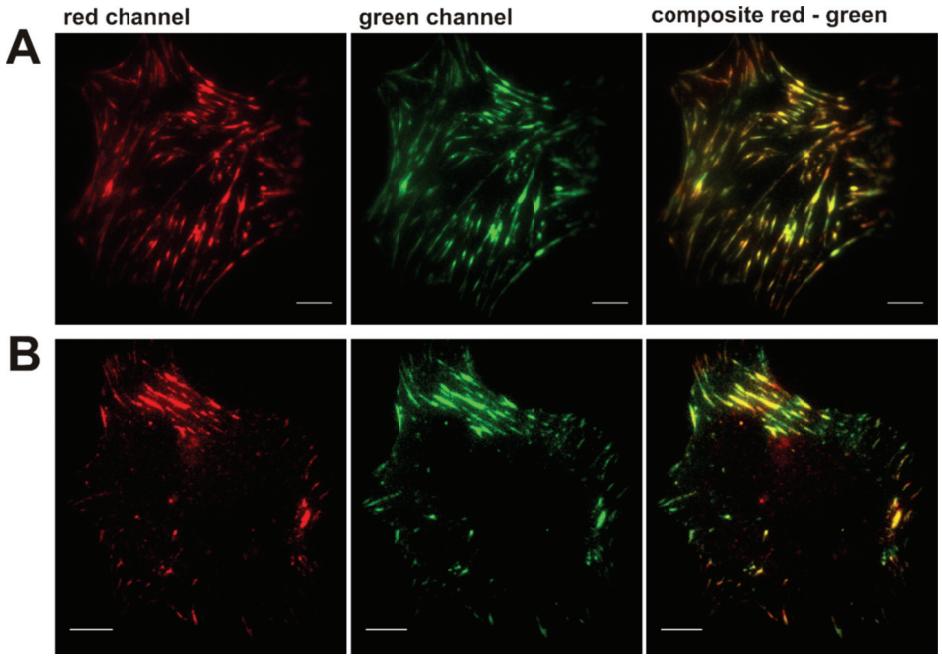

Figure S2. Live cell imaging of Halo- and eDHFR-tagged EGFP-Vcl using TIRF microscopy. MEF Vcl$^{-/-}$ cells were transiently transfected with (A) Halo-EGFP-Vcl (staining: 1 µM Halo-TMR) and (B) eDHFR-EGFP-Vcl (staining: 1 µM TMP-TMR). Live cell images were recorded utilizing a 100x Olympus U apo N TIRF objective and are represented green channel, red channel and as composite images. Scale bars: 5 µm.

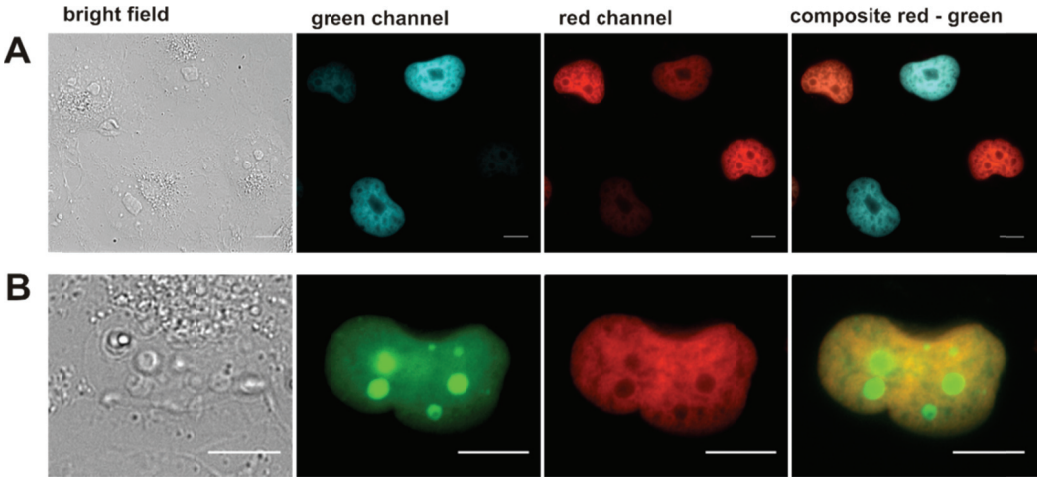

Figure S3. Live cell dual-color imaging of histone proteins H2A and H2B. (A) Dual-color imaging of live COS-7 cells after transient co-overexpression of pmTurquoise2-H2A (green channel) and H2B-Halo (stained with 1 µM Halo-TMR, red channel). (B) Dual-color imaging of live COS-7 cells after transient co-overexpression of tagged histone proteins H2A-Halo and H2B-eDHFR and staining with Halo-TMR (red channel, 1 µM) and TMP-diAcFl (green channel, 1 µM). Images were recorded utilizing a 40x objective and are represented as green channel, red channel and dual-color recordings. Bright field images are shown on the left. Scale bars: 10 µm.

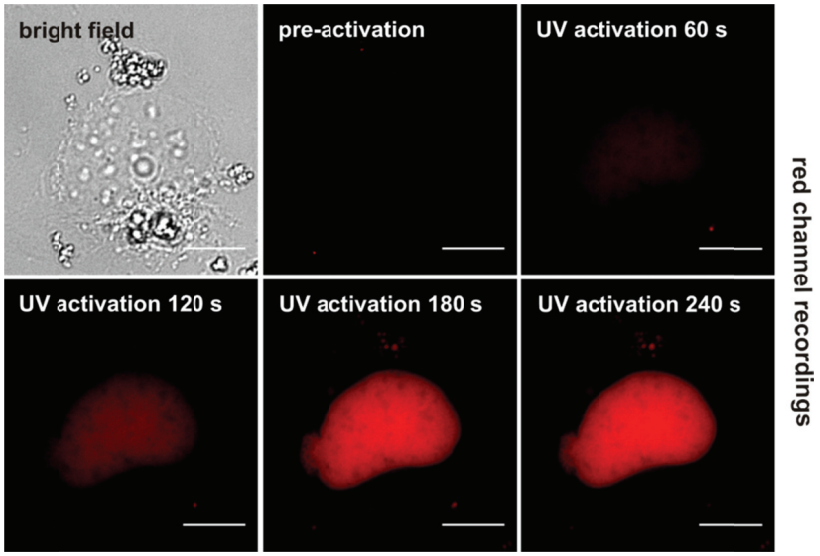

Figure S4. Mono-color photoactivation of histone H2A-localized Halo-PA-Q-Rh in live COS-7 cells. Photoactivation was conducted on live COS-7 cells with transient H2A-Halo overexpression that were stained with Halo-PA-Q-Rh (5 µM). Photoactivation was conducted by exposing the selected ROI to UV light of 352 – 402 nm, 14.5 mW/cm^2. The pre-exposure image was recorded, followed by UV exposure for the indicated time periods. Finally, post-exposure images were acquired. Scale bars: 10 µm.

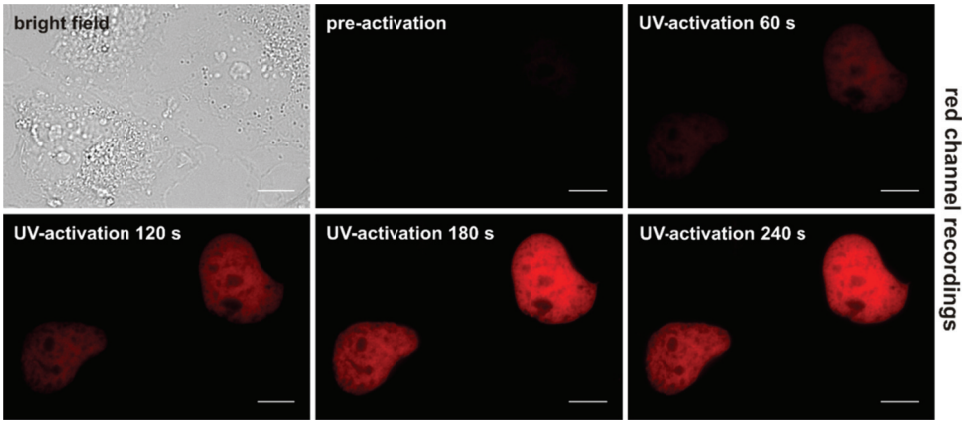

Figure S5. Photoactivation on live COS-7 cells after transient overexpression of H2B-Halo and staining with Halo-PA-Q-Rh (5 µM). Photoactivation was conducted by exposing the selected ROI to UV light of 352 – 402 nm, 14.5 mW/cm^2. The pre-exposure image was recorded, followed by a UV pulse for the indicated time periods. Finally, the respective post-exposure images were acquired. Scale bars: 10 µm.

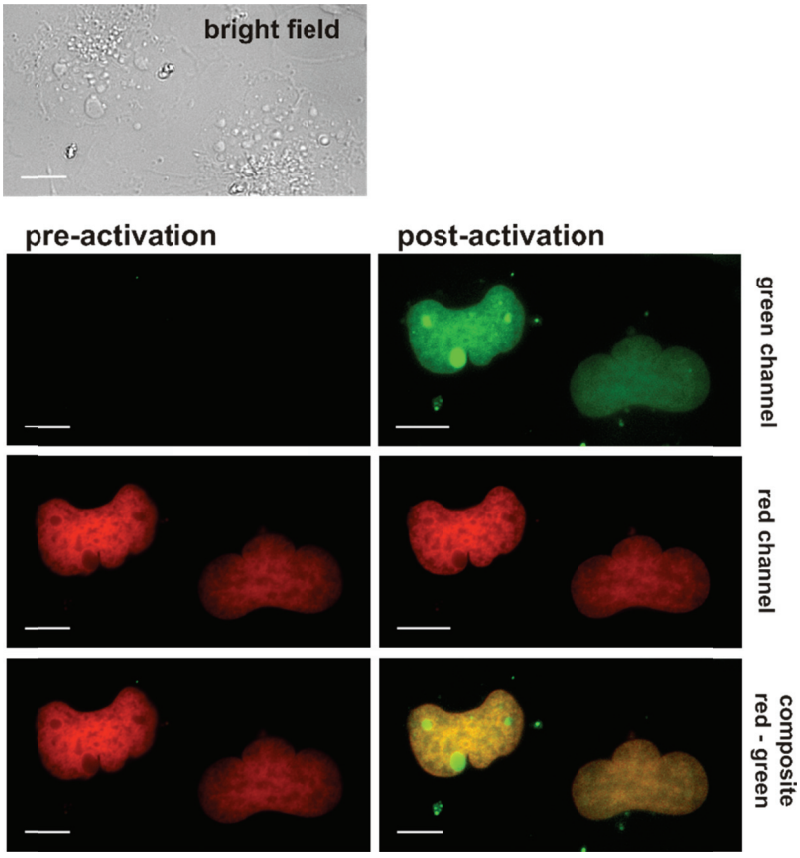

Figure S6. Dual-color imaging (with mono-color photoactivation) of H2B-localized TMP-PA-Fl. Photoactivation was conducted on live COS-7 cells after transient co-overexpression of H2B-eDHFR and H2A-Halo and staining with TMP-PA-Fl (5 µM, green channel) and Halo-TMR (1 µM, red channel). Full activation was detectable after 120 s of UV-exposure. Images were acquired utilizing a 40x objective and are represented as green channel, red channel and dual-color recordings. Photoactivation was conducted by exposing the selected ROI to UV light of 352 – 402 nm, 14.5 mW/cm^2. The pre-exposure image was recorded, followed by a UV pulse for the indicated time periods. Finally, the respective post-exposure images were acquired. Scale bars: 10 µm.

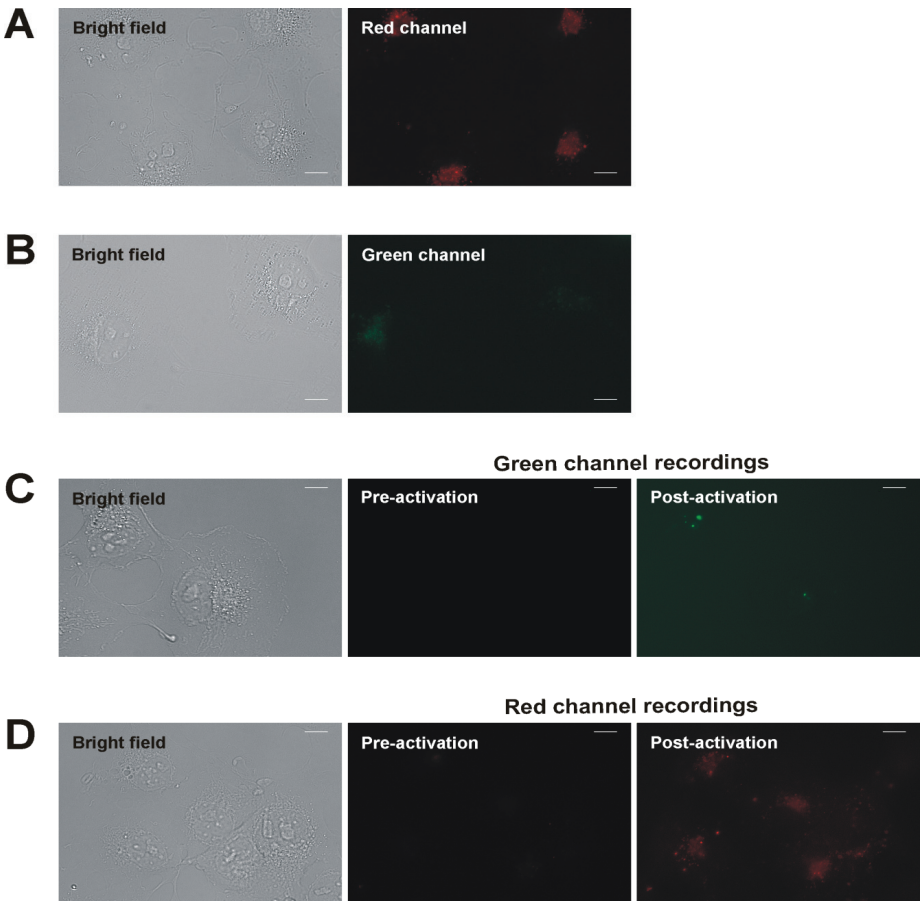

Figure S7. Excluding unspecific binding of (caged) fluorescent dyes in non-transfected live cells. To estimate unspecific binding of fluorescent probes to arbitrary cellular structures, non-transfected live COS-7 cells were stained with TMP-TMR (A) and TMP-diAcFl (B), 1 µM each (bright field and fluorescent channel recordings). Incubation of COS-7 cells with TMP-PA-fluorescein (C) and TMP-PA-Q-Rhodamine (D), 5 µM each. (bright field and fluorescent channel recordings). Photoactivation was conducted by exposing the selected ROI to UV light of 352 – 402 nm, 14.5 mW/cm^2. Scale bars: 10 µm.

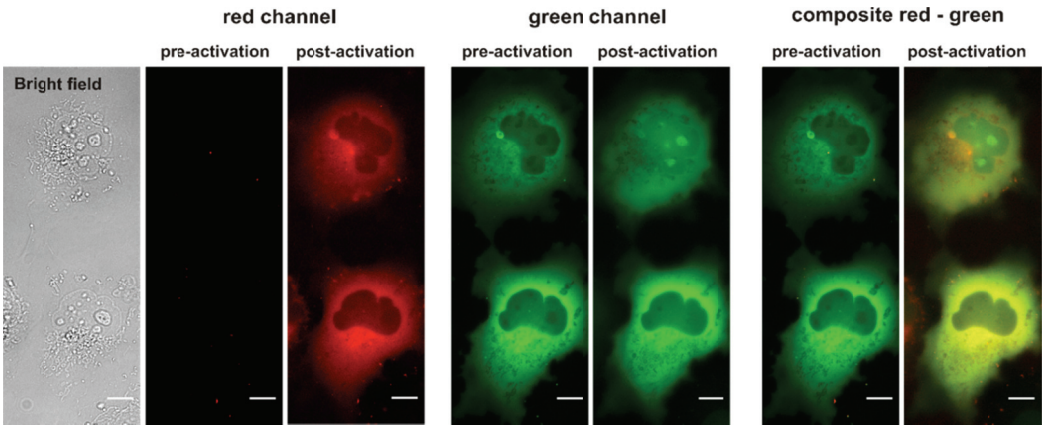

Figure S8. Dual-color photoactivation of nuclear and cytosolic POIs in live COS-7 cells. Halo- and eDHFR-tagged histone H2B and cytosolic eGFP were transiently over-expressed and stained with TMP-PA-Fl and Halo-PA-Q-Rh (5 µM, each). Photoactivation was conducted by exposing the selected ROI to UV light of 352 – 402 nm, 14.5 mW/cm^2, 120 s and is shown in red and green fluorescent channels as well as composite images. Scale bars: 10 µm.

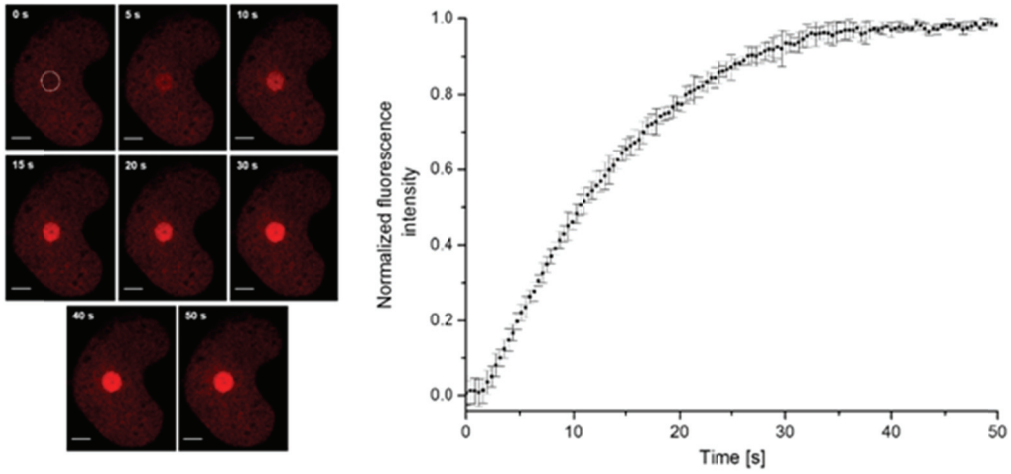

Figure S9. Halo-PA-Q-Rh was localized to H2B-Halo and photoactivation was conducted within circular ROIs (4 µm diameter) that were pre-defined in three live cell nuclei. Repeated activation within one pre-defined spot within the nucleus by laser scanning (405 nm, 60 mW/cm^2, 100% laser power) yielded in increasing fluorescent signal (205 alternating photoactivation and read-out cycles; read-out at λ = 568 nm, 60 mW/cm^2, 15% laser power). As all fluorophores within the pre-defined region were activated, saturation was detected after 40 - 50 s of activation, corresponding to 103 - 128 scan/read-out cycles. No signs of photobleaching were detected in this set up, even though the laser illumination was much stronger, compared to the UV lamp (15 mW/cm^2), applied for photoactivation experiments. Imaging was performed at 37°C on a Perkin Elmer Ultraview VoX spinning disk confocal microscope, using a 63x Zeiss Plan-Apochromat objective. Based on measurements that were conducted on three independent cells, mean values (± standard deviations) were determined as the basis for the plotted curve. Scale bars: 5 µm.

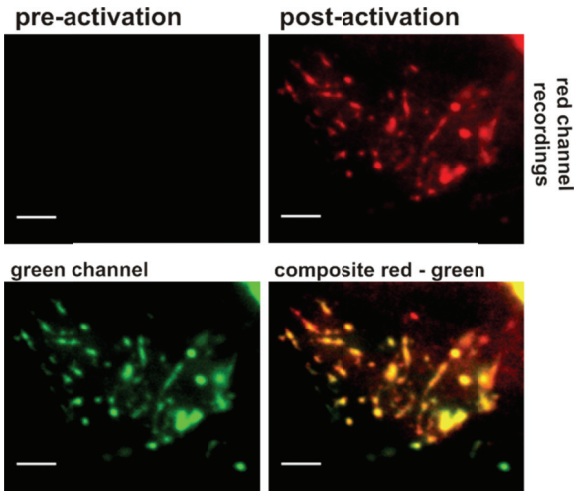

Figure S10. Photoactivation of TMP-PA-Q-Rh, localized to EGFP-Vcl in live cells. MEF Vcl$^{-/-}$ cells were transiently transfected with eDHFR-EGFP-Vcl and stained with TMP-PA-Q-Rh (5 µM). After 50 s of exposure to UV light (405 nm, 60 mW/cm^2, 10% laser power), full activation was detected. Shown are green channel (Vcl-fused EGFP), red channel (TMP-PA-Q-Rh, after 60 s of UV activation) and dual-color recordings. Fluorescent images were acquired utilizing a 100x Olympus U apo N TIRF objective. The pre-exposure image was recorded, followed by a UV pulse. Finally, the respective post-exposure images were acquired. Scale bars: 5 µm.

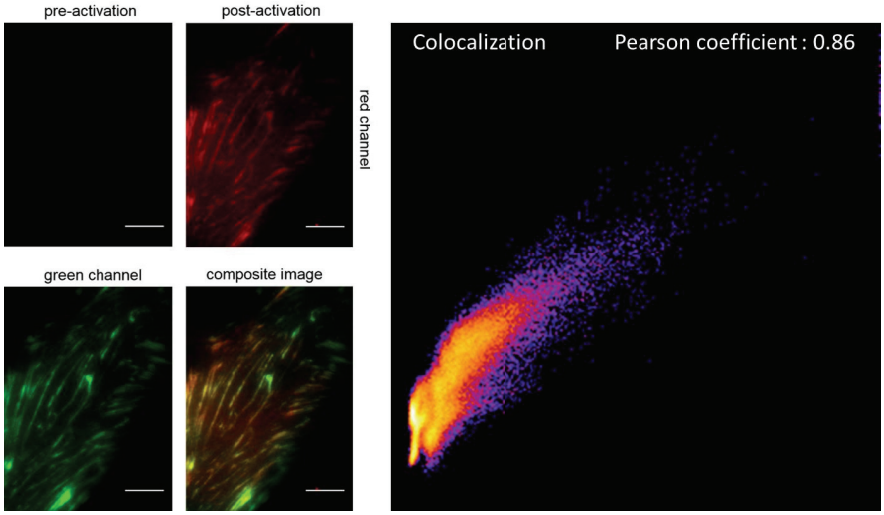

Figure S11. Photoactivation of focal adhesion sites inside live MEF Vcl$^{-/-}$ cells after overexpression of Halo-tagged vinculin-EGFP and staining with Halo-PA-Q-Rh (5 µM). Recordings of post-activation images are shown in the red channel and as composite images. The green channel (lower left) shows the signal from EGFP. The composition image shows good colocalization of both signals from activated Halo-PA-Rh and GFP. Scale bars: 5 µm. Right: Colocalization analysis was performed using Fiji image analysis software tool (using the implemented Coloc 2 for colocalization analysis; http://imagej.net/Coloc_2). The Pearson coeffiecient was determined to 0.86.

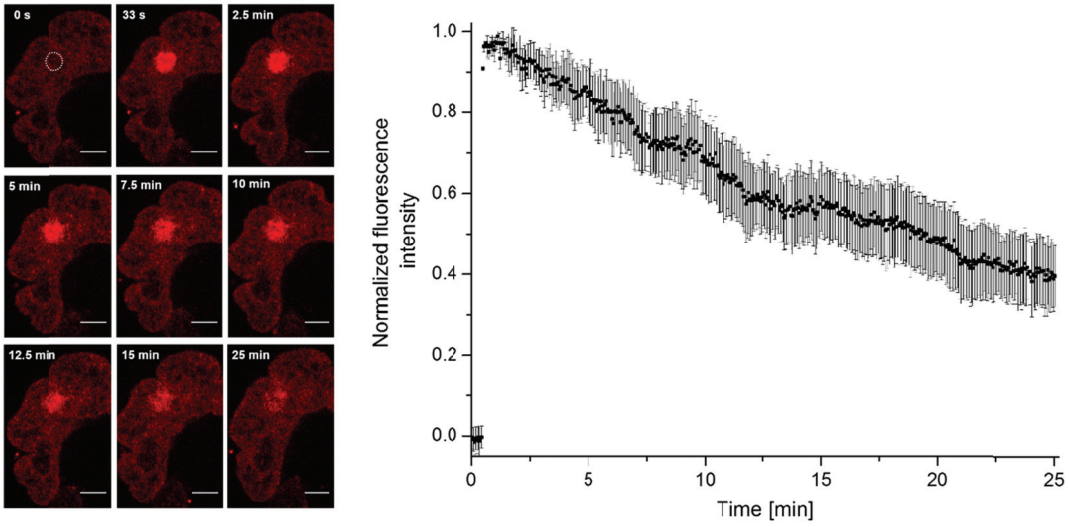

Figure S12 Halo-PA-Q-Rh was localized to H2B-Halo and photoactivation was conducted within circular ROIs (4 µm diameter) that were pre-defined in three live cell nuclei. Repeated activation within the pre-defined spot within the nucleus by laser scanning (405 nm, 60 mW/cm^2, 100% laser power) yielded in increasing fluorescent signal (205 alternating photoactivation and read-out cycles; read-out at λ = 568 nm, 60 mW/cm^2, 15% laser power). Imaging was performed at 37°C on a Perkin Elmer Ultraview VoX spinning disk confocal microscope, using a 63x Zeiss Plan-Apochromat objective. Based on measurements that were conducted on three independent cells, mean values (± standard deviations) were determined as the basis for the plotted curve. Scale bars: 5 µm.

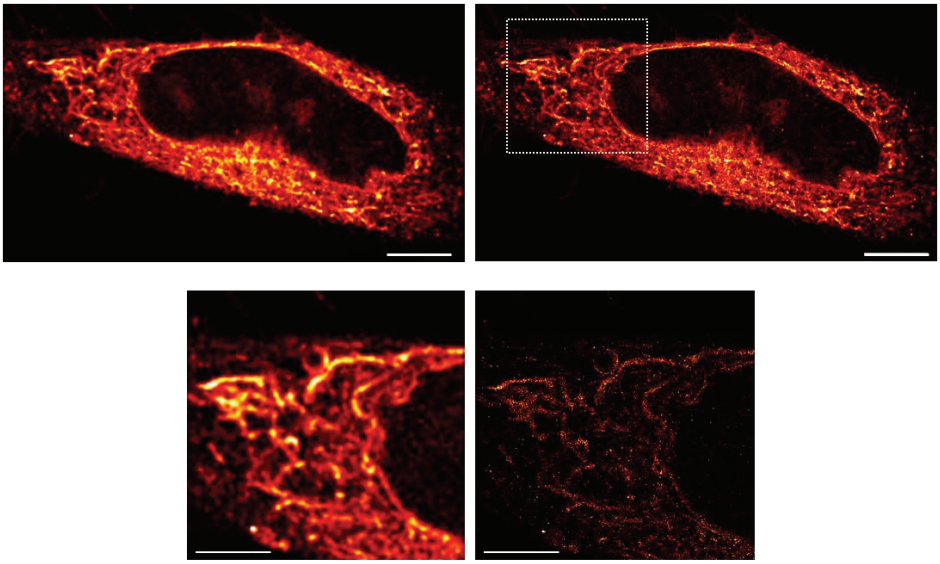

Figure S13. PALMicroscopy on the mitochondrial network in a fixed cell. NIH 3T3 cells were transiently transfected with Tom20-Halo, stained with Halo-PA-Q-Rh and fixed with PFA. The acquired data is represented as diffraction-limited, summed (left) and single-molecule localization (super-resolution) image (right). Structural elements of the mitochondrial network emerged as prominent profiles. Higher magnification views of the boxed region within displayed images (lower panels). Scale bars: 5 µm.

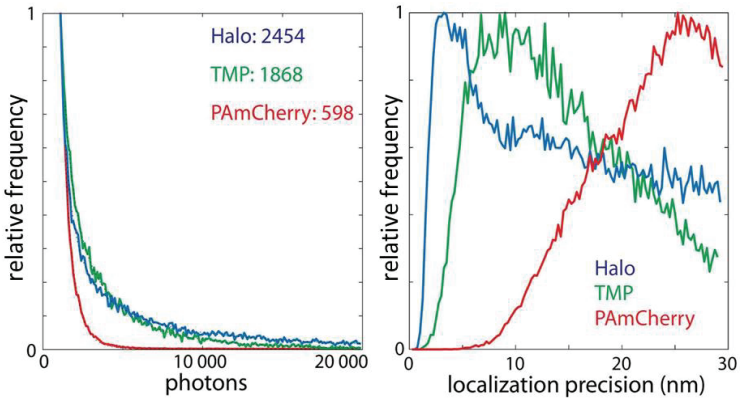

Figure S14 Left: Histograms of photons per single-molecule localization extracted from cell experiments (The numbers denote the mean photon numbers, extracted from a multi-exponential fit in a defined range (1000-20 000 photons) and extrapolation to zero photons). We calculated the mean photon yields for the decaged Halo-Q-PA-Rh (mean photon yield = 2454) and TMP-Q- PA-Rh (mean photon yield = 1868) in comparison to photoactivatable mCherry (PAmCherry) (mean photon yield = 598). Right: The histograms for the localization precision give a localization precision of ~10 nm for Halo-Q-Rh and TMP-Q-Rh and a localization precision of ~25 nm for mCherry.

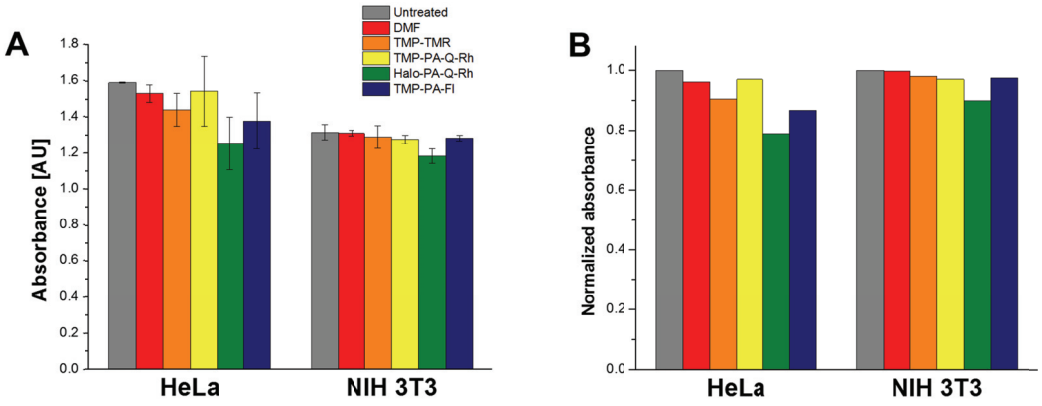

Figure S15. Cell viability analysis after staining with presented dye-constructs with concentrations applied in the live cell experiments (5µM). Absolute values are given in (A). Values, normalized to untreated cells in shown in (B). The same color code was applied for (A) and (B).

10. References

(1) Calloway, N. T.; Choob, M.; Sanz, A.; Sheetz, M. P.; Miller, L. W.; Cornish, V. W. *Chembiochem* **2007**, *8* (7), 767.

(2) Los, G. V; Encell, L. P.; McDougall, M. G.; Hartzell, D. D.; Karassina, N.; Zimprich, C.; Wood, M. G.; Learish, R.; Ohana, R. F.; Urh, M.; Simpson, D.; Mendez, J.; Zimmerman, K.; Otto, P.; Vidugiris, G.; Zhu, J.; Darzins, A.; Klaubert, D. H.; Bulleit, R. F.; Wood, K. V. *ACS Chem. Biol.* **2008**, *3* (6), 373.

(3) Mitchison, T. J.; Sawin, K. E.; Theriot, J. A.; Gee, K.; Mallavarapu, A. *Caged Compounds*; Methods in Enzymology; Elsevier, 1998; Vol. 291.

(4) Haugland, R. P.; Spence, M. T. Z.; Johnson, I. D. *The Handbook: A Guide to Fluorescent Probes and Labeling Technologies*, 10th ed.; Molecular Probes: Eugene, OR.

(5) Joseph R. Lakowicz. *Principles of Fluorescence Spectroscopy*, 3rd ed.; Springer: New York, 2006.

(6) Brismar, H.; Trepte, O.; Ulfhake, B. *J. Histochem. Cytochem.* **1995**, *43* (7), 699.

(7) Johnson, I. *Histochem. J. 30* (3), 123.

(8) Given, Richard S. Conrad, Peter G. Abraham Yousef L, L. Y. I. *Photoremovable Protecting Groups*; CRC Press LLC USA: Boca Raton, 2003.

(9) Il'ichev, Y. V; Schwörer, M. A.; Wirz, J. *J. Am. Chem. Soc.* **2004**, *126* (14), 4581.

(10) Gee, K. R.; Weinberg, E. S.; Kozlowski, D. J. *Bioorg. Med. Chem. Lett.* **2001**, *11* (16), 2181.

(11) Cormack, B. P.; Valdivia, R. H.; Falkow, S. *Gene* **1996**, *173* (1), 33.

(12) Heim, R.; Cubitt, A. B.; Tsien, R. Y. *Nature* **1995**, *373* (6516), 663.

(13) Cubitt, A. B.; Heim, R.; Adams, S. R.; Boyd, A. E.; Gross, L. A.; Tsien, R. Y. *Trends Biochem. Sci.* **1995**, *20* (11), 448.

(14) Yang, T.-T.; Cheng, L.; Kain, S. R. *Nucleic Acids Res.* **1996**, *24* (22), 4592.

(15) Shaner, N. C.; Campbell, R. E.; Steinbach, P. A.; Giepmans, B. N. G.; Palmer, A. E.; Tsien, R. Y. *Nat. Biotechnol.* **2004**, *22* (12), 1567.

(16) Goedhart, J.; von Stetten, D.; Noirclerc-Savoye, M.; Lelimousin, M.; Joosen, L.; Hink, M. A.; van Weeren, L.; Gadella, T. W. J.; Royant, A. *Nat. Commun.* **2012**, *3*, 751.

(17) Wombacher, R.; Heidbreder, M.; van de Linde, S.; Sheetz, M. P.; Heilemann, M.; Cornish, V. W.; Sauer, M. *Nat. Methods* **2010**, *7* (9), 717.

(18) Schindelin, J.; Arganda-Carreras, I.; Frise, E.; Kaynig, V.; Longair, M.; Pietzsch, T.; Preibisch, S.; Rueden, C.; Saalfeld, S.; Schmid, B.; Tinevez, J.-Y.; White, D. J.; Hartenstein, V.; Eliceiri, K.; Tomancak, P.; Cardona, A. *Nat. Methods* **2012**, *9* (7), 676.

(19) Edelstein, A.; Amodaj, N.; Hoover, K.; Vale, R.; Stuurman, N. *Curr. Protoc. Mol. Biol.* **2010**, *Chapter 14*, Unit14.20.

(20) Schoen, I.; Ries, J.; Klotzsch, E.; Ewers, H.; Vogel, V. *Nano Lett.* **2011**, *11* (9), 4008.

(21) Smith, C. S.; Joseph, N.; Rieger, B.; Lidke, K. A. *Nat. Methods* **2010**, *7* (5), 373.